JBUON 2014; 19(3): 705-712
ISSN: 1107-0625, online ISSN: 2241-6293 • www.jbuon.com
E-mail: editorial_office@jbuon.com

ORIGINAL ARTICLE

The antitumor effect and mechanism of taipeinine A, a new C19-diterpenoid alkaloid from *Aconitum taipeicum*, on the HepG2 human hepatocellular carcinoma cell line

Hui Zhang, Zengjun Guo, Ling Han, Xiaojuan You, Ying Xu
School of Pharmacy, Health Science Center, Xi'an Jiaotong University, Xi'an 710061, China

Summary

Purpose: *To investigate whether taipeinine A (JNQ2), a C19-diterpenoid alkaloid prepared from the roots of Aconitum taipeicum, has anticancer effects on hepatocellular carcinoma (HCC) and to study its probable anticancer mechanisms.*

Methods: *JNQ2 activities were assessed on human HCC cell line (HepG2) by proliferative assay, cell cycle arrest assay, apoptosis analysis, cell invasion assay and Western blot analysis.*

Results: *The antitumor activity tests showed that JNQ2 inhibited the proliferation of HepG2 cells in a dose- and time-dependent manner and blocked the cell cycle at the G1/S phase. High dosage of JNQ2 induced significant apoptosis of tumor cells. The invasiveness of HepG2 cells was also inhibited by JNQ2. The mechanism of JNQ2 antitumor effect at the molecular level was presumed to be the upregulation of the protein expression of Bax and Caspase-3 and the downregulation of the protein expression of Bcl-2 and CCND1.*

Conclusion: *Our study suggests that JNQ2 has anticancer effects on HepG2 cells and it is a potential reagent for the treatment of HCC that merits further investigation.*

Key words: *Aconitum taipeicum, antitumor activity, C19-diterpenoid alkaloid, HepG2 cell line*

Introduction

Medicinal plants have played an important role in the treatment of cancer. Alkaloids from medicinal plants are thought to possess important anticancer activities [1-3]. The plant *Aconitum taipeicum* Hand-Mzt. (Ranunculaceae) is an endemic species found in the Qinling Mountain of Shaanxi Province in China. The dried root of *A.taipeicum*, named Jinniuqi, has been used as aconite in the local area for the treatment of rheumatism, hyperkinesia, poisoning, immune disorders and cancer [4-6]. Alkaloids are the main component in Jinniuqi. In a preceding paper, we reported several new alkaloids separated from Jinniuqi and their antileukaemic effects [7,8]. Among them, taipeinine A (Figure 1) was discovered to be the most active compound with IC_{50} lower than 10^{-6} [5]. Therefore, its anticancer properties need to be explored in depth.

HCC is the fifth most common cancer worldwide. About 600,000 patients suffer from HCC annually [9,10]. It is also the third most frequent cause of cancer-related deaths [10]. Although partial hepatectomy and liver transplantation were considered as the main curative treatments for years, only 15% of the patients are good candidates for such treatment modalities [11]. The incidence and mortality rates continue to rise all over the world [12,13] and this may be due in part to the ineffectiveness of the currently available chemotherapeutic drugs. Thus, new therapeutic agents derived from natural products for HCC patients are urgently needed because of their intrinsic advantages [14,15].

Methods

General

Nuclear magnetic resonance (NMR) spectra were recorded on a Bruker Avance III 500 NMR spectrom-

Correspondence to: Zengjun Guo, PhD. School of Pharmacy, Health Science Center, Xi'an Jiaotong University, No. 76, West Yanta Road, Xi'an, Shaanxi 710061, P.R. China. Tel: +86 29 82655133, E-mail: guozj@mail.xjtu.edu.cn
Received: 21/03/2014; Accepted: 03/04/2014

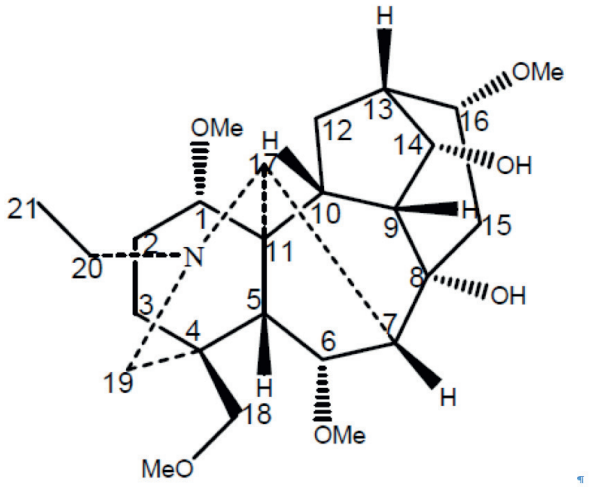

Figure 1. Chemical structure of taipeinine A (JNQ2).

eter (Bruker Corporation, Billerica, MA, USA) with tetramethylsilane as internal standard. High resolution electrospray ionization mass spectrometry (HR-ESI-MS) was conducted using a Micromass Autospec Ultima TOF mass spectrophotometer (Micromass UK Ltd., Altrincham, UK). The melting point was acquired using micro melting point apparatus (Beijing Tech Instrument Co. Ltd., Beijing, China). The materials used for column chromatography (CC) were polyvinyl sulfonic ion exchange resin (H-form, cross linking 001×7, Xi'an Sun resin Technology Ltd., Xi'an, China) and silica gel (SiO2; 200 300 mesh; Qingdao Marine Chemical Factory, Qingdao, China). Thin layer chromatography (TLC) was conducted using glass precoated with silica gel (GF254; 10 40 mm; Qingdao Marine Chemical Factory, Qingdao, China).

Plant material

The roots of *A. taipeicum* were collected from the Qinling Mountain, Shaanxi Province, China, in September 2011 and authenticated by Dr. Juxian Lu, Faculty of Pharmacy, Medical College of Xi'an Jiaotong University (Xi'an, China). The voucher specimen was retained at the Department of Pharmacy, Medical School of Xi'an Jiaotong University for future reference.

Cell culture

Human hepatoma cell line HepG2 was obtained from the Shanghai Institute of Biochemistry and Cell Biology, Chinese Academy of Sciences (Shanghai, China). HepG2 cells ($5.0x10^4$ cells/ml) were cultured in RPMI 1640 supplemented with 10% fetal bovine serum (FBS), containing 2.0 mmol/l glutamine and 1% penicillin streptomycin in 5% CO_2 at 37 °C, and were allowed to adhere for 24 hrs. The experiments were divided into the following 5 groups in the cell proliferation assay (MTT assay): Negative control (dimethyl sulfoxide; DMSO); positive control (15 μmol/l oxaliplatin); low dosage JNQ2 (7.5 μmol/l); middle dosage JNQ2 (15 μmol/l); and high dosage JNQ2 (30 μmol/l). However, the low-dosage group was omitted in other assays due to its low efficiency in the MTT assay.

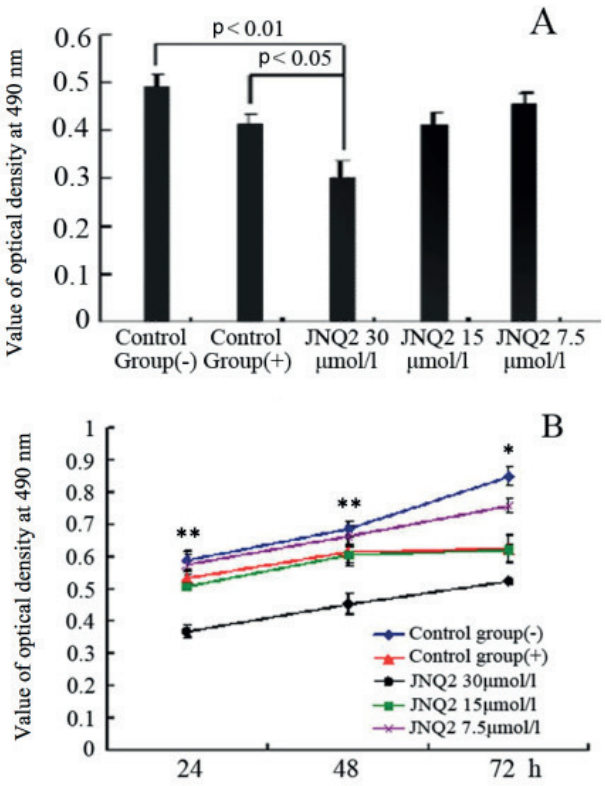

Figure 2. Antiproliferative activity of JNQ2 on HepG2 cells. **A:** Dose-dependent effect of JNQ2 on HepG2 cells for 24hrs when cell viability was determined by the MTT assay; **B:** Time-dependent effect of JNQ2 on HepG2 cells for 3 d when the cell viability was determined by the MTT assay. *p<0.05 compared to positive control, **p<0.01 high dosage group vs positive control.

Extraction and isolation

The dried and powdered roots (2.25 kg) of *A.taipeicum* were filtered with 0.05 mol/l HCl (22 liter) using the method reported previously by Fang and Huo [13]. The filtrate (18 liter) was added to polyvinyl sulfonic ion exchange resin column at a speed of 5 ml/min. Then, the resin column was washed repeatedly with deionized H_2O. The air-dried resin was then alkalized with 10% aqueous $NH_3{\cdot}H_2O$ (0.5 liter) and extracted with ethanol. After evaporation, the total crude alkaloids (14.88 g) were obtained. The crude alkaloids (14 g) were chromatographed over silica gel (550 g) column eluting with $CHCl_3$–MeOH (50:1–3:5) gradient system to give A1–A25 fractions. Taipeinine A (JNQ2) was isolated from fraction A6 by using a silica gel column which was eluted with ethyl acetate–MeOH (23:1).

Taipeinine A (JNQ2): white amorphous powder; melting point 84.8-86.0 °C; ^1H and ^{13}C NMR (500 MHz, $CDCl_3$); Table 1); HR-ESI-MS mass to charge ratio (m/z) 452.3016 ($[M+H]^+$, $C_{25}H_{40}NO_6^+$; calc.452.3011; Table 1).

Table 1. NMR data of JNQ2. δ in PPM, *J* in Hz

No.	δH	δC	*^{1}H-^{1}H COSY*	*HMBC (H→C)*
1	3.00 dd	86.21 d	H-2	C-2, C-10, C-11, C-17, 1-OCH_3
2	1.94 m 2.27 m	25.97 t	H-1, H-3	C-1, C-3
3	1.52 m 1.66 m	35.27 t	H-2	C-1, C-2, C-4, C-18, C-19
4	--	39.44 s	--	--
5	2.21 m	48.65 d	H-6	C-6, C-8, C-10, C-12, C-13, C-14, C-15
6	4.20 d	82.35 d	H-7, H-5	C-4, C-7, C-8, C-17, 6-OCH_3
7	2.04 m	52.59 d	H-6, H-17	C-5, C-6, C-8, C-9, C-15, C-17, C-19
8	--	72.53 s	--	--
9	2.03 m	50.36 d	H-10, H-14	C-1, C-7, C-8, C-10, C-11, C-12, C-15, C-16
10	1.72 m	45.59 d	H-12, H-9	C-1, C-5, C-7, C-8, C-9, C-11, C-12
11	--	50.25 s	--	--
12	1.85 m 1.98 m	28.34 t	H-10, H-13	C-9, C-10, C-11, C-13, C-14, C-16
13	2.30 m	37.88 d	H-12, H-14, H-16	C-10, C-14, C-15, C-16
14	4.12 t (4.5)	75.58 d	H-13, H-9	C-8, C-16
15	2.08 m 2.45 m	38.81 t	H-16	C-7, C-8, C-9, C-13, C-16
16	3.40 m	82.05 d	H-13, H-15	C-8, C-14, 16-OCH_3
17	3.13 s	62.66 d	H-7	C-1, C-6, C-8, C-10, C-11, C-19
18	3.33 ABq 3.71 ABq	80.77 t	--	C-3, C-4, 18-OCH3, C-19
19	2.50 m 2.63 m	53.80 t	--	C-3, C-4, C-5, C-18
21	2.47 m 2.52 m	49.33 t	H-22	C-17, C-19, C-22
22	1.06 t (7.2)	13.75 q	H-21	C-21
1-OCH_3	3.24 s	56.20 q	--	C-1
6-OCH_3	3.34 s	57.33 q	--	C-6
16-OCH_3	3.30 s	56.42 q	--	C-16
18-OCH_3	3.30 s	59.24 q	--	C-18

δ: chemical shift, δH: the chemical shift of proton, δc: the chemical shift of carbon, PPM: part per million (a unit for chemical shift), J: coupling constant, HZ: Hertz (a unit for coupling constant), M: Multiplet, ABQ: AB coupling mode and quartet, T: Triplet, S: Singlet, Q: Quartet, 1H-1H COSY: proton-proton correlation spectroscopy, HMBC (H→C) for proton-carbon correlation spectroscopy (from proton to carbon)

Antiproliferative activity assay for cell viability

HepG2 cells ($2x10^4$ cells/well) were seeded in 96 well plates. Following overnight incubation, test substances were added and the incubation continued at 37 °C in an atmosphere containing 5% CO_2 for 3 days. Subsequently, 20 µl 3 (4,5 Dimethylthiazol 2 yl) 2,5 diphenyltetrazolium bromide (MTT, Sigma Aldrich, St. Louis, MO, USA) solution (5 g/l) was added into each well and incubated for an additional 4 hrs. Supernatants were removed and formazan crystals were dissolved in 200 µl DMSO. The optical density was measured at 490 nm using a POLARstar Optima (BMG Labtech GmbH, Ortenberg, Germany).

Cell cycle and apoptosis analysis

Cell seeding and treatment were the same as in the MTT assay. After 3 days of treatment, cells were harvested by trypsinization and $1×10^6$ cells were counted and used for the analysis. Cells were fixed in ice cold ethanol overnight at 4 °C following washing with PBS. The cells were then washed in PBS again and incubated in 1 ml staining solution (20 µg/ml propidium iodide and 10 U/ml RNase A) for 30 min at room temperature. The cells were examined by fluorescence activated cell sorting (FACS) using a flow cytometer (FACSort; Becton Dickinson, Franklin Lakes, NJ, USA), and the cell cycle populations were determined using ModFit software (Verity Software House, Turramurra, Australia).

For the analysis of apoptotic cell populations, cells were trypsinized and washed in PBS. Staining with Alexa Fluor 647 Annexin V (Invitrogen Life Technologies, Carlsbad, CA, USA) and propidium iodide was performed in 20 mmol/l HEPES buffer (pH 7.4), containing

150 mM NaCl and 2.5 mmol/l $CaCl_2$, for 15 min at room temperature. The cells were examined by FACS using a flow cytometer (FACSort; Becton Dickinson), and the apoptotic populations were determined using ModFit software (Verity Software House).

Cell invasion assay

Cell invasion was evaluated using the Chemicon QCM™ 24 well collagen based cell invasion assay (Millipore, Billerica, MA, USA) according to the manufacturer's instructions. In brief, 0.3 ml serum free medium was added to the interior of each insert to rehydrate the collagen layer for 30 min at room temperature. The medium was then replaced with 0.3 ml prepared serum free cell suspension containing $3.0x10^5$ cells and the corresponding test substances. Medium (500 µl) containing 10% FBS was added to the lower chamber and the cells were incubated for 24 hrs at 37 °C. Following this, all non invaded cells were removed from the interior of the insert and the invaded cells were stained with crystal violet. The stained cells were analyzed on an Olympus fluorescence microscope (BX43; Olympus Corporation, Tokyo, Japan).

Western blot analysis

Cell seeding and treatment were the same as in the MTT assay. After 3 days of treatment, cells were harvested and washed in PBS. Cell protein lysates were separated in 10% SDS polyacrylamide gels and electrophoretically transferred to polyvinylidene difluoride membranes (Roche Diagnostics, Mannheim, Germany). The lysates were then detected using rabbit polyclonal antibodies that were specific for Bcl 2, BAX, caspase 3 and CCND1 (Santa Cruz Biotechnology, Inc., Santa Cruz, CA, USA) and a commercial ECL kit (Pierce Biotechnology, Inc., Rockford, IL, USA). Protein loading was estimated by human anti β actin monoclonal antibody (Santa Cruz Biotechnology, Inc., USA).

Statistics

Statistical analyses were performed by one way ANOVA test followed by Fisher's protected least significant difference *post hoc* test for multiple comparisons using the StatView program (Abacus Concepts, Berkeley, CA, USA). A p-value< 0.05 was considered to indicate a statistically significant difference.

Results

Cell growth inhibition

To evaluate the antitumor role of JNQ2 on human hepatoma cells, antiproliferation and colony formation assays were employed to detect the growth of HepG2 cells at different time points after treatment with JNQ2 in various concentrations. The results showed that JNQ2 exhibited growth inhibitory effect on HepG2 cells in a dose- and time-dependent manner. After 24-h treatment, the optical density value of the high dosage group (JNQ2 30 µmol/l) was significantly lower than that of the negative control group ($p<0.01$), and even significantly lower than that of the positive control group ($p<0.05$) (Figure 2A). The time-effect curve also demonstrated the antiproliferation ability of JNQ2 (Figure 2B). High dosage of JNQ2 (30 µmol/l) kept the cell growth in a very low level during 72 hrs, while the middle dosage (15 µmol/l) did its job as well as the positive control. The colony formation results shown in Figure 3 further confirmed that a high dosage of JNQ2 could inhibit the growth of HepG2 cells. These data suggest that JNQ2 had an inhibitory effect on the proliferation of hepatoma cells.

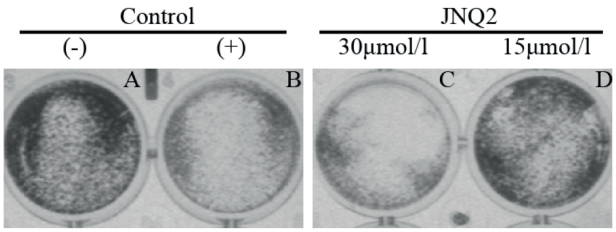

Figure 3. Colony formation of HepG2 cells after treatment with DMSO (**A**), oxaliplatin (**B**) and different concentrations of JNQ2 (**C**: 30µmol/L and **D**: 15µmol/L) for 3 days. Formazan crystals were produced only in the living cells after MTT was added. Therefore, the more the intense density, the more the living cells. In the photo, the negative control group and the low-dosage group showed the heaviest density. The positive control group showed lighter density, while the density of the high-dosage group was the lightest. These findings showed that the high-dosage of JNQ2 inhibited the colony formation of HepG2 cells and its effect was stronger than that of the positive control.

JNQ2-induced G0/G1 cell cycle arrest

To explore the mechanism underlying JNQ2-suppressed cell proliferation, we further investigated the impact of JNQ2 on cell cycle progression by FACS. The results are presented in Figure 4A. After treatment with high and middle dosages of JNQ2, especially the high dosage, the cell cycle shifted from a high S phase to a high G1 phase, together with an accumulation of a G2/M phase population, whereas little effect on the cell cycle was observed in the control groups. These results indicate that JNQ2 blocked the G1/S transition.

JNQ2-induced HepG2 cell apoptosis

To examine the effect of JNQ2 on the apopto-

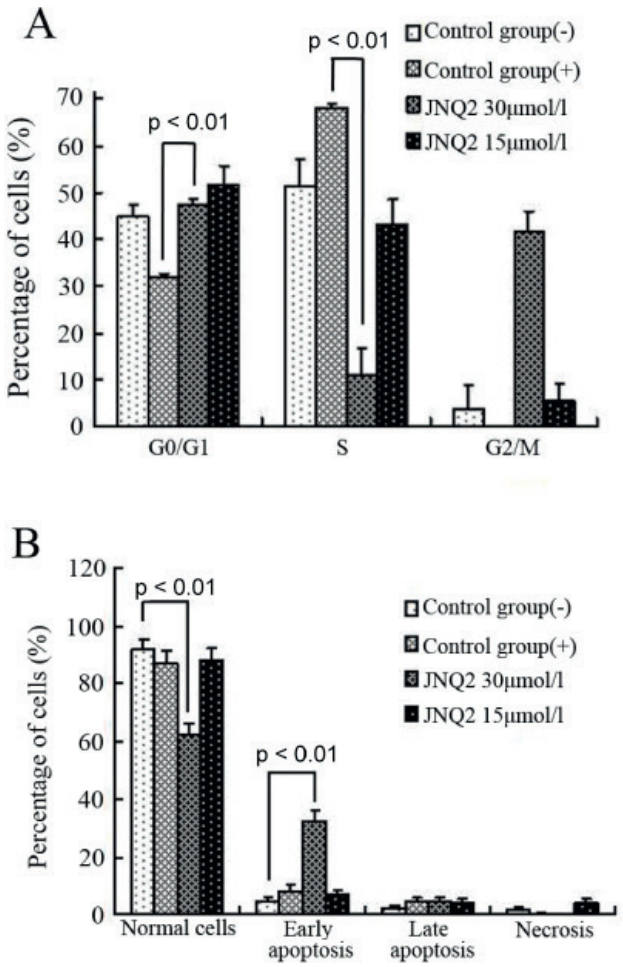

Figure 4. Effect of JNQ2 on the cell cycle and apoptosis of HepG2 cells. **A:** JNQ2-induced G0/G1 cell cycle arrest in HepG2 cells. Effects of JNQ2 on the cell cycle distribution after 24hrs treatment with various concentrations; **B:** JNQ2-induced apoptosis of human hepatoma HepG2 cells after 24hrs of treatment, with data showing the percentages of normal cells, early and late apoptotic cells and necrosis.

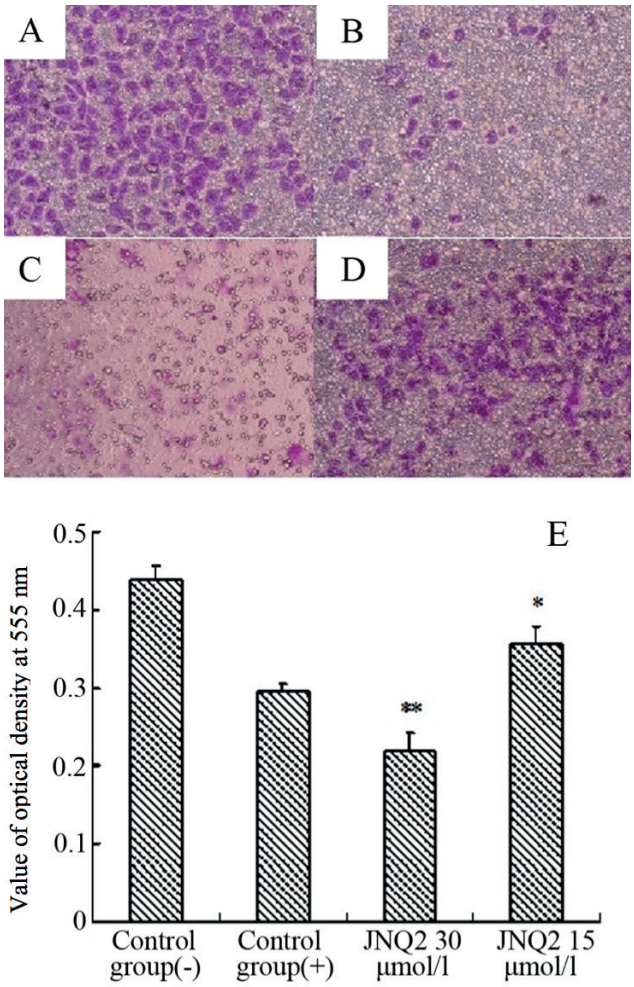

Figure 5. The invasion inhibition effect of JNQ2 on HepG2 cells. **A**: Control group (-). DMSO didn't inhibit the invasion of HepG2 cells, so that there were most crystal violet stained cells in the photo; **B**: Control group (+). The inhibitory effect of oxaliplatin resulted to only some amount of HepG2 cells invasion; **C**: 30μmol/L JNQ2. High-dosage of JNQ2 showed the strongest invasion inhibition effect on HepG2 cells and the cytotoxic effect almost killed all the invading cells. Therefore, the crystal violet stain faded; **D**: 15μmol/L JNQ2. With lower concentration the inhibitory effect of JNQ2 was also reduced, but the amount of the stained cells was still lower than that in the negative control group; **E**: The optical density values of different groups after 24hrs of treatment with JNQ2 or control. In the collagen based cell invasion assay, the invading cells were stained with crystal violet. The more the stained cells, the higher the optical density. The negative control group gave the highest bar, whereas the high-dosage group gave the lowest (**p<0.01 compared to negative control). Lower concentration of JNQ2 shows higher optical density, but still lower than that of the negative control (*p<0.05 compared to negative control).

sis, we treated hepatoma cells with JNQ2 at different concentrations. Compared with the cells treated with control groups, cells treated with JNQ2 at the concentration of 30 μmol/l displayed higher apoptotic rates, whereas the cells that were treated with 15 μmol/l JNQ2 exhibited a similar apoptotic rate as oxaliplatin (Figure 4B). In the 30 μmol/l JNQ2-treated group, the number of cells at the early stage of apoptosis significantly increased (p<0.01, compared with the negative control), while in the positive and 15 μmol/l JNQ2-treated groups the number of cells at the early stage increased slightly and there were no significant differences between them and the negative control group. Cells number at the late stage of positive and JNQ2-treated groups also increased slightly. These data showed that JNQ2 induced apoptosis in human hepatoma cells in a dose-dependent manner.

JNQ2 inhibits cancer invasion in vitro

Cancer invasion is the process in which cells break away from the primary tumor and migrate

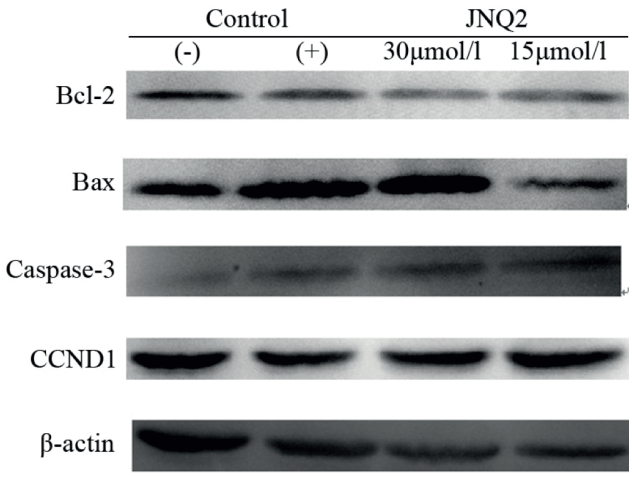

Figure 6. The regulatory effects of JNQ2 on apoptosis-related proteins in HepG2 cells. Blots of BCL-2 and CCND1 in the high-dosage group were clearly smaller than those in the negative control. Meanwhile, blots of BAX and Caspase-3 in the high-dosage group were much larger. The positive control group showed similar expression to that of the high-dosage group, but not that strong. With the reduction of dosage, the influence of JNQ2 to the protein expression was weaken.

through the surrounding tissue. This enables the cancer cells to move into blood vessels and travel through the body, possibly establishing a secondary tumor at another site. To determine whether JNQ2 could inhibit invasion, HepG2 cells were treated with different concentrations of JNQ2, and the control groups were treated separately. Remarkably, the invasion was inhibited by high concentration of JNQ2, whereas migration was not altered in the cells that were treated with the negative control (Figure 5). These results strongly suggest that JNQ2 inhibited the invasion of HepG2 cells.

Western blotting

To clarify the apoptotic mechanism of JNQ2 on HepG2 cells, western blot was performed to examine the protein expression level of Bcl-2, Bax, Caspase-3, and CCND1 (cyclin D1). The cells that were treated with JNQ2 had upregulated Bax and Caspase-3 expression as compared with the negative control cells. This result could explain why JNQ2 inhibited the growth of HepG2 cells, and this function could relate to the mitochondrial pathway-induced apoptosis. Conversely, the protein levels of Bcl-2 and CCND1 were decreased with JNQ2 treatment (Figure 6). The apoptotic effect of JNQ2 was proven by the upregulation of Bax and downregulation of Bcl-2. Based on the G0/G1 arresting capability, the downregulation of CCND1 could provide an explanation. These results suggest that JNQ2 could exhibit its apoptotic effect by upregulation of Bax and Caspase-3 and downregulation of Bcl-2 and CCND1.

Discussion

A. taipeicum has been used in popular medicine for the treatment of rheumatism and hyperkinesias [14]. In previous reports, the plants of the aconitum genus had shown different activities such as antitumor [17,18], analgesic [19,20], anti-inflammatory [21,22], antiepileptic [23], and others. However, no report about the efficiency of *A. taipeicum* in HCC appears in the literature.

Herein, we examined the anticancer activity of a C_{19}-diterpenoid alkaloid taipeinine A, isolated from *A. taipeicum*, in the HepG2 cells. The data presented here showed that JNQ2 could inhibit the proliferation of HepG2 cells. Specifically, JNQ2 affected the cell cycle by arresting the cells in the G0/G1 phase, thus inducing apoptosis. Cancer cell invasion was also inhibited by JNQ2, especially at a high concentration (30 μmol/l). Taken together, these results demonstrate an outstanding antitumor activity of JNQ2. The regulatory effects of JNQ2 upon apoptosis-related protein targets, including Bcl-2, Bax, Caspases-3 and CCND-1, were measured to determine its antitumor mechanism at the molecular level.

As we know, Bcl-2 is an antiapoptotic gene [24-28]. Bcl-2 is closely related to cell apoptosis [29,30], as well as closely associated with the mitochondrion [31,32]. Bax, which can induce cell apoptosis, also belongs to the Bcl-2 family. The ratio of Bcl-2/Bax is the determining factor of antiapoptosis for cells [33]. Our results showed that JNQ2 treatment significantly upregulated the expression of Bax protein and downregulated that of Bcl-2. This suggests that JNQ2 acts on the Bcl-2/Bax genes to exert its apoptotic effect.

Caspase-3, a key regulatory protease upon which many signaling pathways merge for the execution of apoptosis, participates in apoptosis induced by Bcl-2/Bax, p38 and JAK-STAT [34,35]. We detected the protein expression of caspase-3 in HepG2 cells after treatment with JNQ2 and identified the upregulated effect. These results suggest that JNQ2 induced apoptosis of human hepatoma HepG2 cells via the mitochondrial pathway.

CCND1 is a cell cycle control protein that mainly affects G1 progression and G1/S transition.

This cyclin forms a complex with and functions as a regulatory subunit of CDK4 or CDK6, whose activity is required for cell cycle G1/S transition. Its overexpression may contribute to tumorigenesis [36]. Therefore, JNQ2 showed its ability to block the G1/S phase transition by downregulating the expression of CCND1.

Acknowledgement

This work was supported by the National 863 Plan (No. 2012AA02A400), National Natural Science Foundation of China (No.81172957) and the Traditional Chinese Medicine Project of Shaanxi Province (No.13-ZY023).

References

1. Vitaliy OK, Maxim DL, Rostyslav SS. Correlation of the cytotoxic activity of four different alkaloids, from chelidonium majus (greater celandine), with their DNA intercalating properties and ability to induce breaks in the DNA of NK/LY murine lymphoma cells. Cent Eur J Biol 2006;1:2-15.
2. Pierre F, Séverine G. New vinca alkaloids in clinical development. Curr Breast Cancer Rep 2013;5:69-72.
3. Gaur S, Wang YF, Kretzner L et al. Pharmacodynamic and pharmacogenomic study of the nanoparticle conjugate of camptothecin CRLX101 for the treatment of cancer. Nanomedicine: 2014;20:1-10. HTTP://DX.DOI.ORG/10.1016/J.NANO.2014.04.003.
4. Han L, Xu Y, Wu N, Xu W, Guo ZJ. Antitumor compound useful for preparing anti-tumor medicine for treating leukemia, liver cancer, lung cancer, gastric cancer, breast cancer, cervical cancer or prostatic cancer. Xian Jiaotong University, Patent no. CN2010102165686.7, Publication no.CN101851241. State Intellectual Property Office of the P.R.China.
5. Chodoeva A, Bosc JJ, Guillon J. 8-O-Azeloyl-14-benzoylaconine: A new alkaloid from the roots of Aconitum karacolicum Rapcs and its antiproliferative activities. Bioorg Med Chem 2005;13:6493-6501.
6. Lan Z. Collateral-flow-activating pain-relieving ointment of Radix secutidacae for treating affection by dampness. Patent owner: Lan Zihua. Patent no. CN2005101266508.7. Publication no.CNI1814111. State Intellectual Property Office of the P.R.China.
7. Ying X, ZengJun G, Nan W. Two new amide alkaloids with anti-leukaemia activities from Aconitum taipeicum. Fitoterapia 2010;81:1091-1093.
8. Zengjun G, Ying X, Hui Z et al. New alkaloids from Aconitum taipaicum and their cytotoxic activities. Nat Pro Res 2013; DOI:10.1080/14786419.2013.861832.
9. Lau WY, Lai ECH. Hepatocellular carcinoma: current management and recent advances. HBPD Int 2008;7:237-257.
10. Shiraha H, Yamamoto K, Namba M. Human hepatocyte carcinogenesis (Review). Int J Oncol 2013;42:1133-1138.
11. Ma SM, Jiao BZ, Liu X et al. Approach to radiation therapy in hepatocellular carcinoma. Cancer Treat Rev 2010;36:157-163.
12. Altekruse SF, McGlynn KA, Reichman ME. Hepatocellular Carcinoma: Incidence, Mortality, and Survival Trends in the United States from 1975 to 2005. J Clin Oncol 2009;27:1485-1491.
13. Agnello F, Salvaggio G, Cabibbo G. Imaging appearance of treated hepatocellular carcinoma. World J Hepatol 2013;5:417-424.
14. Lee KH. Discovery and development of natural product-derived chemotherapeutic agents based on a medicinal chemistry approach. J Nat Prod 2010;73:500-516.
15. Burgess DJ. Dangerous micromanagement. Nat Rev Cancer 2010;10:664-644.
16. Fang QC, Huo ZM. Methods carried on the extraction and separation of total alkaloids from plants with the ion exchange resin. Acta Pharm Sin 1966;13:577-588.
17. Li E, Chen XY. Study on the anticancer effect of Aconitine on KBv200. Chin J Inform TCM 2004;11:103-105.
18. Duan JY, Liu XP, Li Q. An experimental study of the antitumor effect of Aconitum Szeehnyianum Gay. Shenzhen J Integr Tradit Chin Western Med 1998;8:3-15.
19. Kang L, Yue SW, Wang XL, Fang M. The analgesic effect and mechanism of the transdermal iontophoresis of aconitine on arthrophlogosis in a rat model. Chin J Phys Med Rehabil 2005;27:733-736.
20. Taki M, Niitu K, Omiya Y et al. 8-O-cinnamoylneoline, a new alkaloid from the flower buds of Aconitum carmichaeli and its toxic and analgesic activities. Plant Medica 2003;69:800-803.
21. Shi HB, Zhou CC, Li YZ et al. Anti-inflammatory effect of Aconitines. Chin J Chin Mater Med 1990;15:46-50.
22. Huang YM, Li CS, Zhang ZJ et al. Anti-inflammation and pharmacodynamics of Wutou injection in mice. Chin Pharm J 2006;41:1249-1251.
23. Ameri A. The effects of Aconitum alkaloids on the central nervous system. Prog Neurobiol 1998;56:211-235.
24. O'Neill JW, Hockenbery DM. Bcl-2-related proteins as drug targets. Curr Med Chem 2003;10:1553-1562.
25. Cory S, Adams JM. Killing cancer cells by flipping the Bcl-2/Bax switch. Cancer Cell 2005;8:5-6.
26. Fathi NA, Hussein MR, Hassan HI et al. Glomerular expression and elevated serum Bcl-2 and Fas proteins in lupus nephritis: preliminary findings. Clin Exp Immunol 2006;146:339-343.

27. Zhang R, Xue YY, Lu SD et al. Bcl-2 enhances neurogenesis and inhibits apoptosis of newborn neurons in adult rat brain following a transient middle cerebral artery occlusion. Neurobiol Dis 2006;24:345-356.
28. Karlnoski R, Wilcock D, Dickey C et al. Up-regulation of Bcl-2 in APP transgenic mice is associated with neuroprotection. Neurobiol Dis 2007;25:179-188.
29. Bernas T, Asem EK, Robinson JP et al. Confocal fluorescence imaging of photosensitized DNA denaturation in cell nuclei. Photochem Photobiol 2005;81:960-969.
30. Yoshida A, Takemura H, Inoue H et al. Inhibition of glutathione synthesis overcomes Bcl-2-mediated topoisomerase inhibitor resistance and induces non-apoptotic cell death via mitochondrial-independent pathway. Cancer Res 2006;66:5772-5780.
31. Degli EM. Mitochondria in apoptosis: past, present and future. Biochem Soc Trans 2004;32:493-495.
32. Dias N, Bailly C. Drugs targeting mitochondrial functions to control tumor cell growth. Biochem Pharmacol 2005;70:1-12.
33. Haupts U, Haupts C, Oesterhelt D. The photoreceptor sensory rhodopsin-I as a 2-photon driven proton pump. Proc Natl Acad Sci USA 1995;92:3834-3838.
34. Dassé E, Bridoux L, Baranek T et al. Tissue inhibitor of metalloproteinase-1 promotes hematopoietic differentiation via caspase-3 upstream the MEKK1/MEK6/p38alpha pathway. Leukemia 2007;21:595-603.
35. Lanvin O, Gouilleux F, Mullié C et al. Interleukin-7 induces apoptosis of 697 pre-B cells expressing dominant-negative forms of STAT5: evidence for caspase-dependent and -independent mechanisms. Oncogene 2004;23:3040-3047.
36. Guo L, Xue TY, Xu W, Gao JZ. Matrine promotes G0/G1 arrest and downregulates cyclin D1 expression in human rhabdomyosarcoma cells. Panminerva Med 2013;55:291-296.